Grain-Boundary Fluctuations in Two-Dimensional Colloidal Crystals

Thomas O. E. Skinner,* Dirk G. A. L. Aarts, and Roel P. A. Dullens

Department of Chemistry, Physical and Theoretical Chemistry Laboratory, University of Oxford, South Parks Road, Oxford OX1 3QZ, United Kingdom

(Received 30 July 2010; published 13 October 2010)

We study grain-boundary fluctuations in two-dimensional colloidal crystals in real space and time using video microscopy. The experimentally obtained static and dynamic correlation functions are very well described by expressions obtained using capillary wave theory. This directly leads to values for the interfacial stiffness and the interface mobility, the key parameters in curvature-driven grain-boundary migration. Furthermore, we show that the average grain-boundary position exhibits a one-dimensional random walk as recently suggested by computer simulations [Z. T. Trautt, M. Upmanyu, and A. Karma, Science **314**, 632 (2006)]. The interface mobility determined from the mean-square displacement of the average grain-boundary position is in good agreement with values inferred from grain-boundary fluctuations.

DOI: 10.1103/PhysRevLett.105.168301 PACS numbers: 82.70.Dd, 68.35.−p, 05.70.Np

The physical properties of many materials such as semiconductors, metals, and ceramics are determined by their microstructure, the presence of defects, and the grain size distribution [1–3]. Defects such as dislocations and grain boundaries can, for instance, arise due to freezing-in during crystal growth or as a result of stress on the crystal. The presence of different crystallites is particularly important for the mechanical properties, as the grain size is directly related to the strength of materials [4,5]. Also, processes like grain growth, phase transformations, and recrystallization are heavily influenced by the motion and evolution of grain boundaries [3,6].

Grain-boundary migration is a direct consequence of the competition between thermal energy, which causes any interface to be microscopically rough, and the tendency to minimize the grain-boundary curvature and surface area. The kinetics of such curvature-driven interfaces are governed by two parameters: the grain-boundary stiffness Γ and the interface mobility M. The grain-boundary stiffness is the sum of the interfacial tension γ and the second derivative of the interfacial tension with respect to the orientation of the grain boundary $\ddot{\gamma}$. The stiffness is well known to be important in solidification where its orientation dependence helps control the growth and specific orientation of dendrites [7]. The grain-boundary mobility is the proportionality constant that relates the grain-boundary velocity v to the curvature κ and the grain-boundary stiffness: $v = M\Gamma\kappa$ [1]. The grain-boundary stiffness and mobility are therefore the key parameters that govern the structure and dynamics of curvature-driven grain growth.

There are various ways to determine the grain-boundary stiffness and mobility in experiments [8,9] and simulations [10–13]. However, especially for the measurement of the interface mobility, these methods usually require significant driving forces. Computer simulations have demonstrated that equilibrium grain-boundary fluctuations provide an elegant zero-driving force route to both the grain-boundary stiffness and mobility [7,11]. Grain-boundary fluctuations can be expressed as a sum of thermally excited capillary waves [14] where the displacements are represented in reciprocal space as the Fourier components $A(k)$. From the equipartition theorem it follows that, in the small slope ($\frac{dh}{dx} \ll 1$) and long wavelength limit, the equilibrium fluctuation spectrum of a rough interface is given by [15,16]

$$\langle |A(k)|^2 \rangle = \frac{k_B T}{L\Gamma k^2}. \quad (1)$$

Here, the angular brackets denote a configurational average, L is the interface length, and $k_B T$ is the thermal energy.

It has recently been shown that interface fluctuations are experimentally very well accessible in colloidal systems [17,18]. While much of the current experimental knowledge on grain boundaries has been inferred from detailed high-resolution transmission electron microscopy studies [9,19–21], directly accessing the interface fluctuations in atomic grain boundaries is problematic due to the short time and length scales [22]. So far only computer simulations have employed capillary fluctuations to extract the stiffness and mobility of atomic grain boundaries [11,23–26]. Here, we exploit the increased time and length scales of a colloidal model system [27–30] to directly monitor the grain-boundary fluctuations in a colloidal crystal. Using capillary wave theory, we determine the grain-boundary stiffness and mobility from the real space correlations functions. We also determine the grain-boundary mobility from the diffusive motion of the mean grain-boundary position, thereby experimentally confirming this approach suggested by computer simulations [12].

We use colloidal melamine-formaldehyde spheres with a diameter of 2.7 μm (Microparticles GmbH).

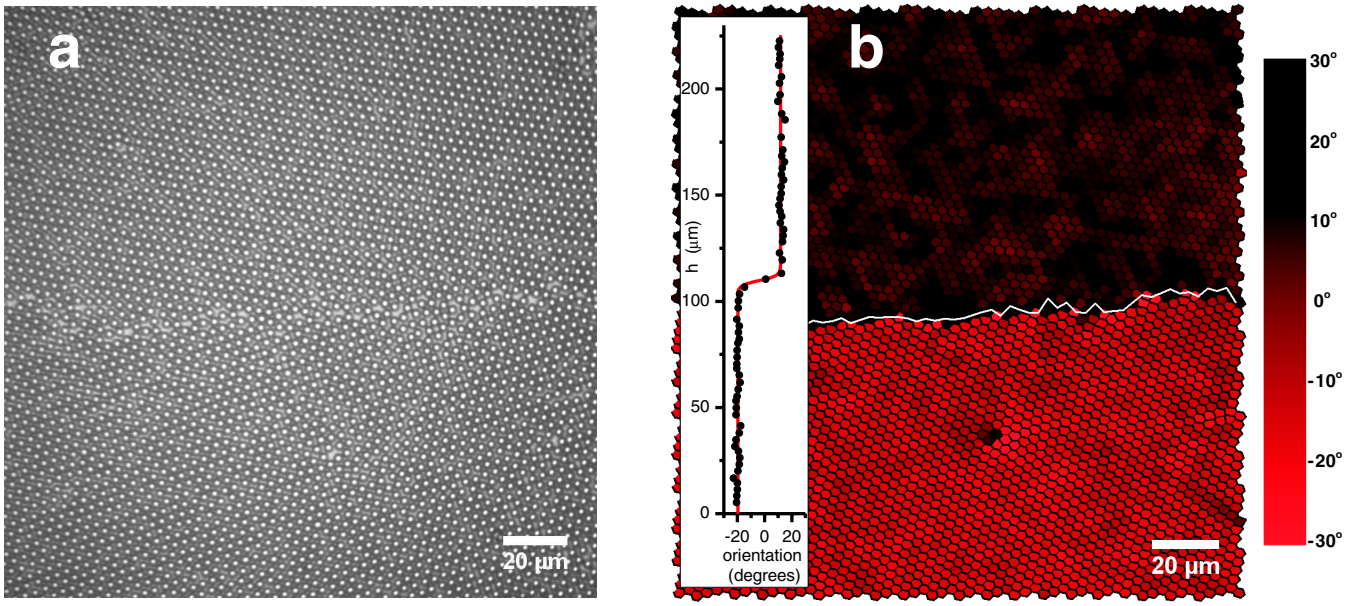

FIG. 1 (color online). (a) An example of a grain boundary in a two-dimensional colloidal crystal of 2.7 μm diameter melamine-formaldehyde particles. (b) An orientation Voronoi plot corresponding to the image in (a). Each Voronoi cell corresponds to a particle and its color represents the local orientation of the particle as indicated by the color bar. The two different crystallites and the interface are easily recognized. Inset: Fitting a tangent hyperbolic to the local orientation as a function of the distance to the interface, the interface is localized for each bin. The complete interface is then found as shown by the solid line in (b).

The particles are dispersed in water and interact through a short-range screened Coulomb potential. The particles are contained in a 200 μm thick glass sample cell, and after sedimentation a two-dimensional hexagonal colloidal crystal is formed as shown in Fig. 1(a). The number density in the crystal is 0.11 $\mu\mathrm{m}^{-2}$. As the particle size is much greater than the gravitational height, the out-of-plane fluctuations of the particles are negligible. Using optical video microscopy long image stacks of colloidal grain boundaries [Fig. 1(a)] of length $L \sim 200$ μm are recorded at typically 0.5 Hz for several hours. Standard particle tracking software is used to find the particle coordinates [31].

To find the interface a local orientation parameter $\Phi(i)$ is assigned to each particle i. To this end, first the N nearest neighbor coordinates $\vec{r}_j$ of every particle i are found using a Delaunay triangulation. Next, the angle $\theta_j = \tan^{-1}(\vec{r}_j - \vec{r}_i)$, with $-\pi \leq \theta_j \leq \pi$, subtended from the central particle i to each of its nearest neighbors j is obtained. The orientation parameter is then obtained as $\Phi(i) = \frac{1}{N}\sum_j \theta_j$. Each frame is subsequently split into bins of size approximately the particle diameter and perpendicular to the interface direction. The local orientation parameter is then plotted across the interface as shown in Fig. 1(b). A tangent-hyperbolic fit to this profile gives the interface position for each bin. As a result, the interface height h as a function of the distance along the interface x and time t is then obtained: $h(x, t)$. To analyze the fluctuations, the interface averaged over all frames is subtracted: $h'(x, t) = h(x, t) - \langle h(x)\rangle_t$.

The grain-boundary fluctuations are analyzed in real space by constructing the time-dependent height-height correlation function:

$$g_h(x, t) = \langle [h'(x_0, t_0)][h'(x_0 + x, t_0 + t)]\rangle. \quad (2)$$

The static correlation function $g_h(x)$ averaged over all x_0 and time t is expressed as $g_h(x, t = 0) = \langle h'(x_0) h'(x_0 + x)\rangle$ and is shown in Fig. 2(a). The correlation function shows a rapid monotonic decay and approaches zero around 20 μm. To extract the grain-boundary stiffness from the static correlation function, we note that the interface position $h(x, t)$ can be expressed as $h(x, t) = \sum_k A(k, t)e^{ikx}$. In other words, Fourier transforming Eq. (1) yields an expression for $g_h(x)$. The sum is converted to an integral over all k, where we assume that $k_{\mathrm{min}} = 0$ and $k_{\mathrm{max}} = \infty$. Note that only the even real part of e^{ikx} remains. To avoid divergence of the integral as $k \to 0$, a lateral correlation length ξ is introduced which ensures a smooth long wavelength cutoff [32,33]:

$$g_h(x) = \frac{k_B T}{\pi\Gamma}\int_0^\infty \frac{1}{k^2 + \xi^{-2}}\cos(kx)dk = \frac{k_B T}{2\Gamma}\xi e^{-x/\xi}. \quad (3)$$

Figure 2 shows excellent agreement between the experimental data and theory. Fitting Eq. (3) to the experimental static correlation function gives a grain-boundary stiffness of 1.7×10^{-15} J m^{-1} and a correlation length of 4.9 μm. The fact that $L \gg \xi$ confirms that the fluctuation spectrum is not affected by the finite length of the grain boundary. For comparison, we also computed the stiffness from the power spectrum using Eq. (1), plotting $\langle |A(k)|^2\rangle$ as

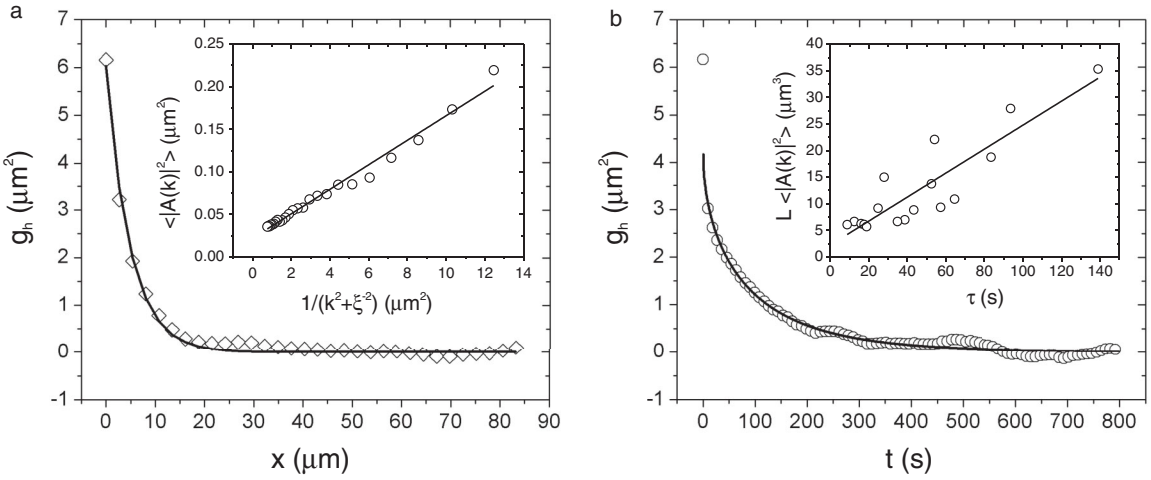

FIG. 2. (a) The static height-height correlation function $g_h(x)$: experimental data (symbols) and a fit (solid line) according to Eq. (3). The inset shows the power spectrum from which the stiffness is deduced using Eq. (1). (b) The dynamic correlation function $g_h(t)$: experimental data (symbols) and a fit (solid line) according to Eq. (5). The inset shows a plot of the amplitudes of the interface fluctuations versus their corresponding decay times, from which the mobility is found as explained in the text.

a function of $1/k^2$ as shown in the inset of Fig. 2(a). The value of 1.8×10^{-15} J m^{-1} compares very well with the stiffness obtained using our real space approach. Alternatively, the function may be approximated to the one point self-correlation function, the mean-square interface width, as $\langle h^2 \rangle = g_h(0) = k_B T \xi / 2\Gamma$. Using a correlation length of 4.9 μm indeed gives a consistent stiffness of 1.6×10^{-15} J m^{-1}.

The dynamic correlation function is given by $g_h(x = 0, t) = \langle h'(t_0) h'(t_0 + t) \rangle$ and is shown in Fig. 2(b). Each Fourier mode decays exponentially according to

$$\langle A(k, 0) A^*(k, t) \rangle = \langle |A(k)|^2 \rangle e^{-M\Gamma k^2 t}, \tag{4}$$

with a decay constant $\tau = 1/M\Gamma k^2$ that depends on both the grain-boundary stiffness Γ and the mobility M [13]. Subsequently, substituting Eq. (1) into Eq. (4), Fourier transforming, and converting the sum to an integral results in

$$g_h(t) = \frac{2k_B T}{\pi\Gamma} \int_0^\infty \frac{1}{k^2 + \xi^{-2}} e^{-M\Gamma(k^2 + \xi^{-2})t} dk = \frac{k_B T \xi}{\Gamma} \operatorname{erfc}\left(\frac{(\Gamma M t)^{1/2}}{\xi} \right), \tag{5}$$

where $\operatorname{erfc}(t)$ is the complementary error function. Hence, in contrast to the static correlation function, the dynamic correlation function directly yields the grain-boundary stiffness Γ *and* the mobility M. Consistently, the one point self-correlation function reduces to the mean-square interface width $k_B T \xi / 2\Gamma$. Equation (5) describes the experimental data points accurately, and from the fit a grain-boundary stiffness and mobility of 4.8×10^{-15} J m^{-1} and 28 m^3/J s are extracted, respectively. Here, we used $\xi = 4.9 \times 10^{-6}$ m as found from $g_h(x)$. The value for the stiffness is in good agreement with the value obtained from the static correlation function and the power spectrum. However, we expect the dynamic method to be more accurate as this is not limited by the length of the interface.

We also determined the mobility from the decay of the Fourier modes [11]: substituting Eq. (1) into $\tau = 1/M\Gamma k^2$ leads to $L\langle |A(k)|^2 \rangle = k_B T M \tau$. Subsequently plotting $L\langle |A(k)|^2 \rangle$ as a function of τ [see inset Fig. 2(b)] results in a mobility of $M = 55$ m^3/J s, which compares well to the grain-boundary mobility obtained from the dynamic height-height correlation function.

Recent computer simulations suggested that the grain-boundary mobility can also be extracted using the fluctuation-dissipation theorem in the limit of zero-driving force [12]. The approach is based on the average interface position $\bar{h} = \frac{1}{L} \int_0^L h(x, t) dx$ performing a one-dimensional (1D) random walk. This is the interface analog of the Stokes-Einstein relation for 1D diffusion of a Brownian particle: $\langle \bar{h}^2 \rangle = 2Dt$, where the diffusion constant D is directly proportional to the grain-boundary mobility M [12],

$$D = \frac{M k_B T}{L}. \tag{6}$$

Figure 3(a) shows a typical trajectory of the average interface position $\bar{h}$ in time, and a representative probability distribution corresponding to a time interval of 200 s is shown in Fig. 3(b). The Gaussian shape of the distribution confirms that the interface performs a 1D random walk and is therefore consistent with the method suggested in [12]. The grain-boundary mobility is subsequently extracted from the time dependence of the mean-square displacement, Fig. 3(b). We find a grain-boundary mobility of 70 m^3/J s, which again is in excellent agreement with the mobility obtained from the dynamic correlation function. Note that data for times smaller than the Brownian time ($\sim$ 10 s) are not taken into account.

Because values for the grain-boundary stiffness and mobility in colloidal crystals have not been reported to the best of our knowledge, we discuss our results in the light of two- and three-dimensional computer simulations of atomic grain boundaries. Typical stiffnesses reported for

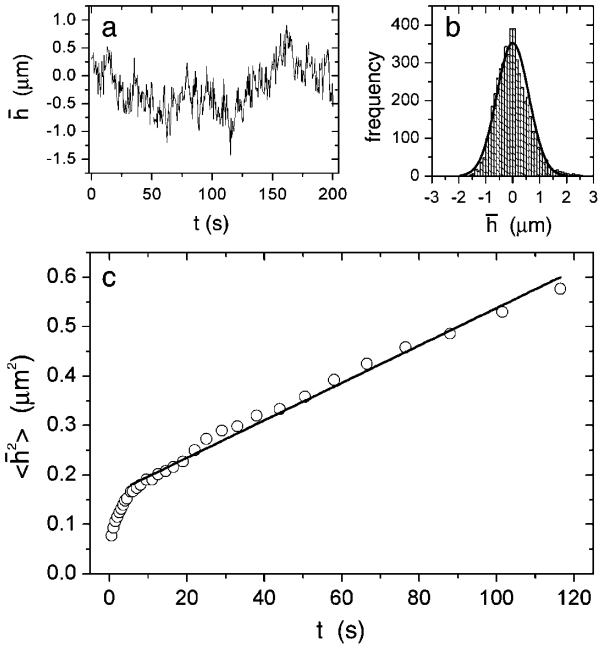

FIG. 3. (a) A typical trajectory of the average interface $\bar{h}$ position as a function of time. (b) The probability distribution of $\bar{h}$ for a time interval of 200 s. The solid line is a Gaussian fit to the distribution. (c) The mean-square displacement of $\bar{h}$ as a function of the time. The solid line is a linear fit to the data (for times larger than the Brownian time).

2D and 3D atomic simulations are of the order of 10^{-11} J/m [25] and 1 J/m^2 [11], respectively. These values are consistent with the stiffness scaling as $\sim k_B T/l_c$ in 2D and $\sim k_B T/l_c^2$ in 3D, where l_c is the characteristic length scale, which for atomic systems is $\sim$1 Å. Applying this to a 2D colloidal system with $l_c \sim 1$ μm, a stiffness of $\sim 10^{-15}$ J m^{-1} is expected, which is in very good agreement with our findings. Similarly, typical mobilities found in 3D atomic simulations (no 2D data available) range from $\sim 10^{-7}$ to 10^{-9} m^4/(J s) [11,12]. This can be understood using $M \sim l_c^4/(k_B T t_c)$, with t_c the characteristic time scale which for atomic systems is $\sim$1 ps [12]. In 2D this reduces to $M \sim l_c^3/(k_B T t_c)$, so that for our 2D colloidal system with $t_c \sim 10$ s a mobility of $\sim$100 m^3/(J s) is expected. Again, this is in excellent agreement with the values determined from the dynamic correlation function and the random walk analysis. This simple scaling analysis shows the robustness and the applicability of our real space analysis for the investigation of grain-boundary fluctuations and the direct measurement of the grain-boundary stiffness and mobility. We believe that this approach will also prove very useful in simulation studies and in further studies addressing the effect of impurities and confinement on the structure and mobility of grain boundaries using colloids as a condensed matter model system.

We thank Gert Aarts, Anna Maciolek, and Klaus Mecke for useful discussions and EPSRC for financial support.

*thomas.skinner@chem.ox.ac.uk

[1] C. Herring, *The Physics of Powder Metallurgy* (McGraw-Hill, New York, 1951).
[2] J. P. Hirth and J. Lothe, *Theory of Dislocations* (Wiley, New York, 1982), 2nd ed.
[3] J. M. Howe, *Interfaces in Materials* (Wiley, New York, 1997).
[4] S. Yip, Nature (London) **391**, 532 (1998).
[5] H. Van Swygenhoven, Science **296**, 66 (2002).
[6] T. Zykova-Timan, R. E. Rozas, J. Horbach, and K. Binder, J. Phys. Condens. Matter **21**, 464102 (2009).
[7] J. J. Hoyt, M. Asta, and A. Karma, Mater. Sci. Eng., R **41**, 121 (2003).
[8] N. Eustathopoulos, Int. Met. Rev. **28**, 189 (1983).
[9] Y. Huang and F. J. Humphreys, Acta Mater. **47**, 2259 (1999).
[10] M. Asta, C. Beckermann, A. Karma, W. Kurz, R. Napolitano, M. Plapp, G. Purdy, M. Rappaz, and R. Trivedi, Acta Mater. **57**, 941 (2009).
[11] S. M. Foiles and J. Hoyt, Acta Mater. **54**, 3351 (2006).
[12] Z. T. Trautt, M. Upmanyu, and A. Karma, Science **314**, 632 (2006).
[13] J. Hoyt, Z. Trautt, and M. Upmanyu, Math. Comput. Simul. **80**, 1382 (2010).
[14] L. Mandelstam, Ann. Phys. (Leipzig) **346**, 609 (1913).
[15] M. P. A. Fisher, D. S. Fisher, and J. D. Weeks, Phys. Rev. Lett. **48**, 368 (1982).
[16] D. Bedeaux and J. D. Weeks, J. Chem. Phys. **82**, 972 (1985).
[17] D. G. A. L. Aarts, M. Schmidt, and H. N. W. Lekkerkerker, Science **304**, 847 (2004).
[18] J. Hernández-Guzmán and E. R. Weeks, Proc. Natl. Acad. Sci. U.S.A. **106**, 15 198 (2009).
[19] D. L. Medlin, S. M. Foiles, and D. Cohen, Acta Mater. **49**, 3689 (2001).
[20] S. Lee, Mater. Lett. **57**, 3779 (2003).
[21] K. Merkle, L. Thompson, and F. Phillipp, Interface Sci. **12**, 277 (2004).
[22] M. I. Mendelev and D. J. Srolovitz, Model. Simul. Mater. Sci. Eng. **10**, R79 (2002).
[23] A. E. Lobkovsky, A. Karma, M. I. Mendelev, M. Haataja, and D. J. Srolovitz, Acta Mater. **52**, 285 (2004).
[24] H. Zhang, M. I. Mendelev, and D. J. Srolovitz, Acta Mater. **52**, 2569 (2004).
[25] Z. Trautt and M. Upmanyu, Scr. Mater. **52**, 1175 (2005).
[26] K. G. F. Janssens, D. Olmstead, E. A. Holm, S. M. Foiles, S. J. Plimpton, and P. M. Derlet, Nature Mater. **5**, 124 (2006).
[27] A. R. Bausch, M. J. Bowick, A. Cacciuto, A. D. Dinsmore, M. F. Hsu, D. R. Nelson, M. G. Nikolaides, A. Travesset, and D. A. Weitz, Science **299**, 1716 (2003).
[28] P. Lipowsky, M. J. Bowick, J. H. Meinke, D. R. Nelson, and A. R. Bausch, Nature Mater. **4**, 407 (2005).
[29] A. M. Alsayed, M. F. Islam, J. Zhang, P. J. Collings, and A. G. Yodh, Science **309**, 1207 (2005).
[30] V. W. d. Villeneuve, L. Derendorp, D. Verboekend, E. C. Vermolen, W. K. Kegel, H. N. Lekkerkerker, and R. P. Dullens, Soft Matter **5**, 2448 (2009).
[31] J. C. Crocker and D. G. Grier, J. Colloid Interface Sci. **179**, 298 (1996).
[32] K. Binder, M. Müller, F. Schmid, and A. Werner, J. Comput.-Aided Mater. Des. **4**, 137 (1998).
[33] A. Werner, F. Schmid, M. Müller, and K. Binder, J. Chem. Phys. **107**, 8175 (1997).